ELSEVIER

Journal of Alloys and Compounds 408–412 (2006) 711–716

Journal of ALLOYS AND COMPOUNDS

www.elsevier.com/locate/jallcom

Synthesis and luminescence property of Eu^{3+}/ZrO_2 thin film by the liquid phase deposition method

Kentaro Kuratani [a], Minoru Mizuhata [b], Akihiko Kajinami [b], Shigehito Deki [b,c,*]

[a] *Department of Molecular Science, Graduate School of Science and Technology, Kobe University, 1-1, Rokkodai-cho, Nada, Kobe 657-8501, Japan*

[b] *Department of Chemical Science and Engineering, Faculty of Engineering, Kobe University, 1-1, Rokkodai-cho, Nada, Kobe 657-8501, Japan*

[c] *Department of Molecular Science and Materials Engineering, Graduate School of Science and Technology, Kobe University, 1-1, Rokkodai-cho, Nada, Kobe 657-8501, Japan*

Received 7 August 2004; received in revised form 10 December 2004; accepted 13 January 2005
Available online 26 May 2005

Abstract

Transparent Eu^{3+}-doped metal oxide thin films have been directly fabricated on various kinds of substrates by the liquid phase deposition (LPD) method. The stabilization of Eu^{3+} ion in the LPD reaction solution, containing F^- anions, was successfully achieved by using diethylenetriaminepentaacetic acid (DTPA) as a masking regent. The structural and luminescence properties for the deposited films were analyzed. The deposited films consisted of nano-sized spherical particles. The formation of solid-solution was confirmed from the film after annealing above 800 °C. The strong excitation peak due to charge transfer (CT) band was observed. After being annealed at 900 °C, the deposited film shows characteristic strong emission from Eu^{3+}, $^5D_0 \rightarrow {}^7F_2$, under CT band excitation.

Keywords: Thin film; Chemical synthesis; Crystal structure and symmetry; Luminescence

1. Introduction

Rare earth (Ln) ion based compounds have attracted much attention since they have large practical and potential applications in many fields, such as high-performance luminescent devices [1–3], magnets [4,5], catalysts [6–8] and so on. These characteristics are based on the electronic, optical, and chemical properties arising from their 4f electrons. Among the rare earth elements, Eu^{3+} is particularly interesting for the luminescence because the main emission band is centered at 611 nm, which is one of the three primary colors. Therefore, Eu^{3+} has been intensively studied as a luminescent activator in various host matrices. For developing effective luminescence device, material which has much lower phonon energy should be selected as host material because the high phonon energy of the host lattice are responsible for nonradiative relaxation. SiO_2 matrix (phonon energy; 1100 cm^{-1}) is widely used as a host due to their high transparency in visible region. However, the network structure of SiO_2 makes it impossible to introduce high content of dopant without clustering which leads to concentration quenching of emission.

ZrO_2 is one of the candidates for the substitution of SiO_2 as host matrix of Eu^{3+} ion due to its chemical and photochemical stability, high refractive index and low phonon energy. The stretching mode of the ZrO_2 is about 470 cm^{-1}, which is much lower than for Al_2O_3 (870 cm^{-1}) or SiO_2 (1100 cm^{-1}). Several preparation techniques have been proposed to fabricate ZrO_2 thin films by dry processes, such as sputtering [9,10], chemical vapor deposition [11], and atomic layer deposition [12–14]. Among these methods, the solution based technique is a promising and powerful method for fabricating ZrO_2 thin films due to its simplicity and low energy consumption.

* Corresponding author. Tel.: +81 78 803 6160; fax: +81 78 803 6160.
E-mail address: deki@kobe-u.ac.jp (S. Deki).

0925-8388/$ – see front matter © 2005 Elsevier B.V. All rights reserved.
doi:10.1016/j.jallcom.2005.01.075

Recently, we have reported a novel preparation method of metal oxide thin films by using hydrolysis of metal-fluoro complex and reactor in aqueous solution, which we call the liquid phase deposition (LPD) method [15]. In this process, the following equilibrium reaction is presumed:

$$MF_x^{(x-2n)-} + H_2O \leftrightarrow MO_x + HF \quad (1)$$

$$H_3BO_3 + 4HF \leftrightarrow BF_4^- + H_3O^+ + 2H_2O \quad (2a)$$

$$Al + 6HF \leftrightarrow H_3AlF_6 + \frac{3}{2}H_2 \quad (2b)$$

The equilibrium reaction (1) shifts to the right-hand side by the addition of boric acid or aluminum-metal, which readily react with F^- ions to form more stable complex ions [Eqs. (2a) and (2b)] [16–18].

In general, rare-earth ions readily react with F^- ions and form insoluble LnF_3 (Ln; rare-earth) compound. In our previous studies, an organic ligand, such as EDTA, had been used as masking reagent for Ln^{3+} ions to prevent the formation of LnF_3 precipitates in the LPD solution [19]. In this paper, we report a new preparation method and luminescence property of transparent Eu^{3+}-doped ZrO_2 thin films by the LPD method. The stabilization of Eu^{3+} ions can be achieved by using diethylenetriaminepentaacetic acid (DTPA) as a masking reagent for Eu^{3+} ions. We also show that the emission intensity from the film excited under UV light is about 100 times larger than that of the film excited at 396 nm.

2. Experimental procedure

For preparation of ZrO_2 thin films, 3.0 mol dm^{-3} hexafluorozirconic acid (H_2ZrF_6; Morita Chemical Co. Ltd.) were used as a starting material. As F^- ion scavenger, aluminum-metal with a surface area of 48 cm^2 was used for the deposition. DTPA, as a masking reagent for Eu^{3+} ion, was dissolved into ion-exchanged water at a concentration of 0.2 mol dm^{-3}. Pure Eu_2O_3 was dissolved into 10% hydrochloride solution. With the aqueous ammonium solution, pH value of the aqueous $EuCl_3$ solution was controlled at ca. 5. The concentration of Eu^{3+} ion in this solution was 0.2 mol dm^{-3}. The aqueous DTPA solution was mixed with the aqueous $EuCl_3$ solution. The molar ratio of Eu^{3+}: DTPA was 1:1. The aqueous solution containing H_2ZrF_6 and Eu^{3+}/DTPA complex and aluminum-metal plate was used as a reaction solution. Final concentration of H_2ZrF_6 in the reaction solution was 0.06 mol dm^{-3}. The concentration of Eu^{3+}/DTPA complex added into the reaction solution was constant (2 mmol dm^{-3}). The 11 mol% Eu^{3+}-doped ZrO_2 thin films could be obtained in this condition. Soda-lime glass, fused silica glass and Si wafer were used as substrate. Substrates were cleaned ultrasonically and then immersed into the treatment solution for 24 h at 30 °C. These substrates were then removed from reaction solution, washed with distilled water and then dried at room temperature overnight. Subsequently, the films were heat-treated for 1 h at various temperatures.

Atomic force microscopy (AFM: SPI-300, Seiko Instruments Int.) working in tapping mode was employed to investigate surface morphology of the films. Optical transmittance of the films was measured by UV–vis spectrometer (Hitachi; U-3000) in the range from 400 to 800 nm. X-ray diffraction (XRD) analysis for the films was carried out on a Rigaku RINT-2100 diffractometer equipped with thin film attachment. Raman spectra were measured with Jobin-Yvon U-1000 KX double monochromator. The emission line at 488.0 nm from Ar^+ ion laser was used as excitation source. Luminescence measurements were performed by using a FP-6500 spectrofluorometer (JASCO).

3. Results and discussion

Fig. 1 shows surface morphology of the deposited Eu^{3+}-doped ZrO_2 thin films annealed at various temperatures. The images in Fig. 1 clearly show that the small particles deposit all over the substrate, indicating that the oxide thin film deposits on surface of substrate. For as-deposited film (Fig. 1(a)), the film consists of densely packed small spherical particles with mean size of ca. 80 nm in diameter. We can see that the film has crack-free and uniform structure. This homogeneous structure is one of the features of the deposited thin film by the LPD method because the film formation in this process relies on direct deposition of metal oxide on immersed substrate in the reaction solution. This film formation process is quite different from other solution-based film formation process such as sol–gel method. With the increase of annealing temperature, the surface morphology was varied remarkably. After being annealed at 500 °C (Fig. 1(b)), the aggregation of particles is confirmed and the average particle size reaches about 120 nm in diameter. No shape change of particles is found from images. This aggregation of particles can also be observed with the increase of annealing temperature. The particle sizes of the films after being annealed at 700 and 900 °C are 150 and 200 nm, respectively.

High optical transmission in visible region is required for luminescence materials to obtain the effective emission. Optical transmission spectra of the Eu^{3+}-doped ZrO_2 thin film before (solid-line) and after (dashed-line) being annealed at 900 °C is shown in Fig. 2. The film was deposited onto fused silica glass. The as-deposited film shows more than 90% transmittance in the region from 400 to 800 nm. After being annealed at 900 °C, the film also shows high transparency (more than 70% transmittance), although slight decrease of the transmittance, caused by scattering of visible light by aggregated particles, is observed in Fig. 2. From these results, it is concluded that Eu^{3+}-doped ZrO_2 thin film fabricated by the LPD method have high transparency before and after being annealed at 900 °C because the film has dense and homogeneous structure formed by nanometer-sized small particles.

Fig. 3 shows XRD patterns of the Eu^{3+}-doped ZrO_2 thin films annealed at various temperatures. The inset in Fig. 3 is an enlarged pattern in the range of $28^\circ < 2\theta < 32^\circ$. The as-

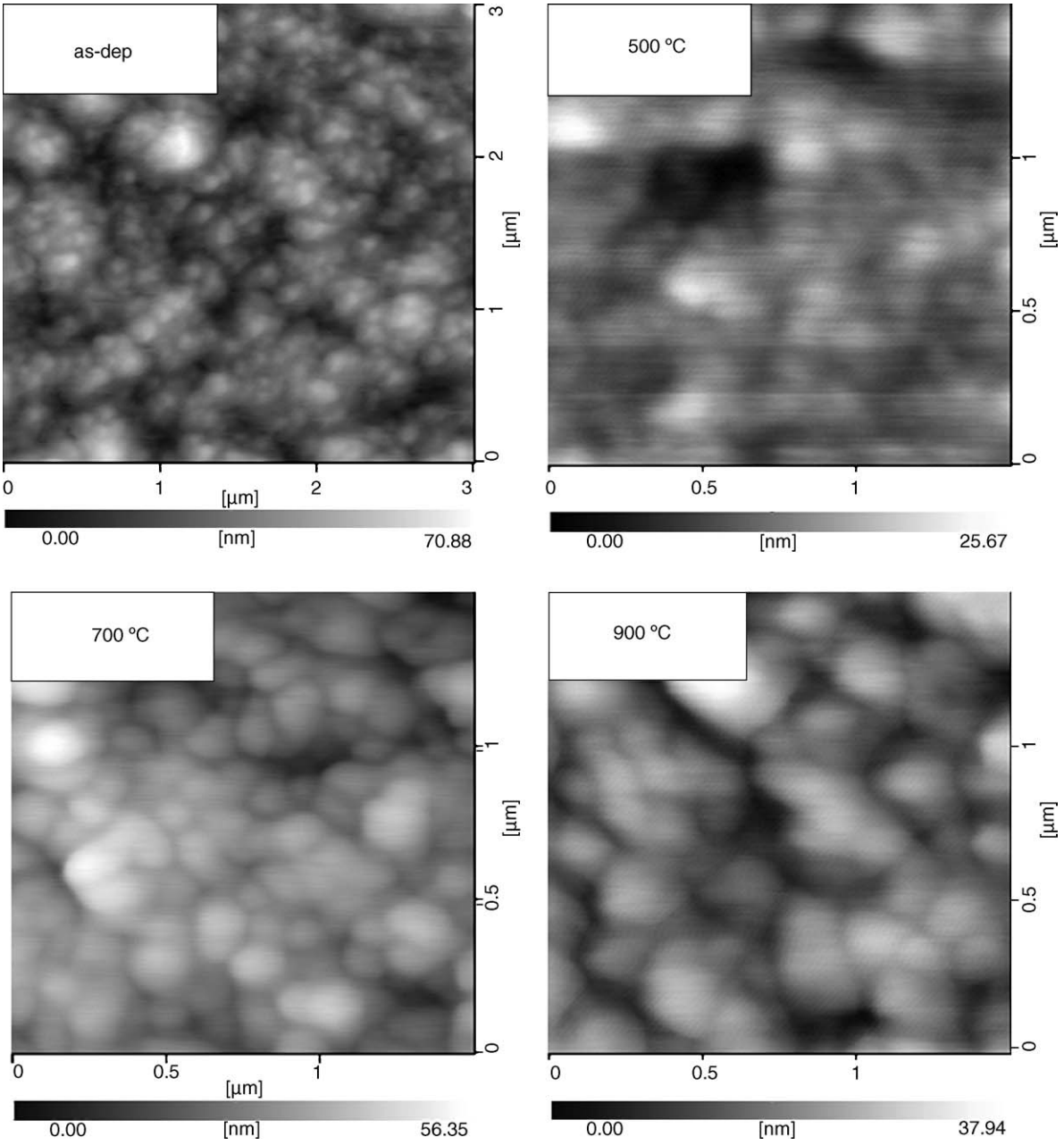

Fig. 1. AFM images of the deposited Eu^{3+}-doped ZrO_2 thin film annealed at various temperatures.

deposited film had amorphous structure (not shown here). After the film was annealed above 500 °C, the peaks assigned to tetragonal or cubic structure appear in the pattern, and no peaks assigned to monoclinic phase can be confirmed. It is difficult to distinguish between tetragonal and cubic phase of ZrO_2 from XRD patterns because most of XRD reflection peaks of cubic and tetragonal phase of ZrO_2 overlap. The determination of phase structure of the film was carried out by Raman spectroscopy and the result will be demonstrated later. The peak intensity of the film increases with the increase of annealing temperature. The crystallite size estimated by the basis of Scherrer equation also increases from 27.3 to 30.7 nm, indicating improvements in crystallinity at higher temperature. After being annealed above 800 °C, as shown in the inset, slight shift of diffraction peaks to lower diffraction angle can be observed, suggesting the substitution of Zr^{4+} (ionic radius; 87 pm) lattice site in the film by Eu^{3+} (ionic radius; 98 pm) ions and formation of solid-solution.

Raman spectroscopy is a very useful tool to distinguish between tetragonal and cubic phase of ZrO_2. Raman spectra of the film after being annealed at (a) 700 °C and (b) 900 °C are shown in Fig. 4. The strong peaks could be confirmed at 520 cm^{-1} in both spectra, which was due to Si substrate. It can be seen in Fig. 4(a) that the main bands are at 261, 330, 466, 612, and 636 cm^{-1} (indicated by solid-arrows). These bands are assigned to the Raman-active vibration modes for

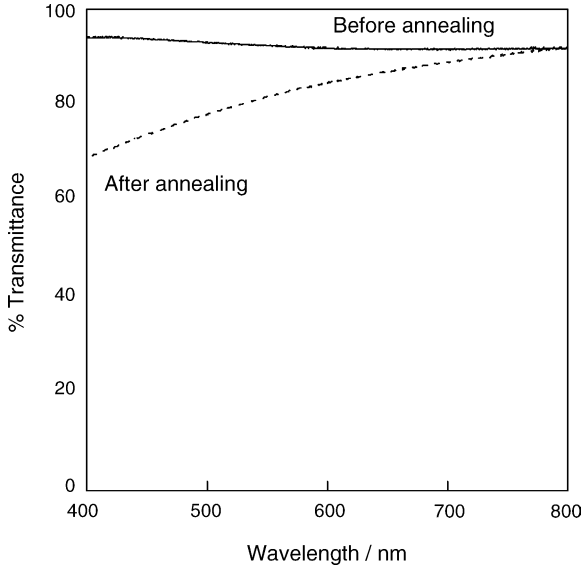

Fig. 2. Optical transmittance spectra of the Eu^{3+}-doped ZrO_2 thin film before and after annealing at 900 °C.

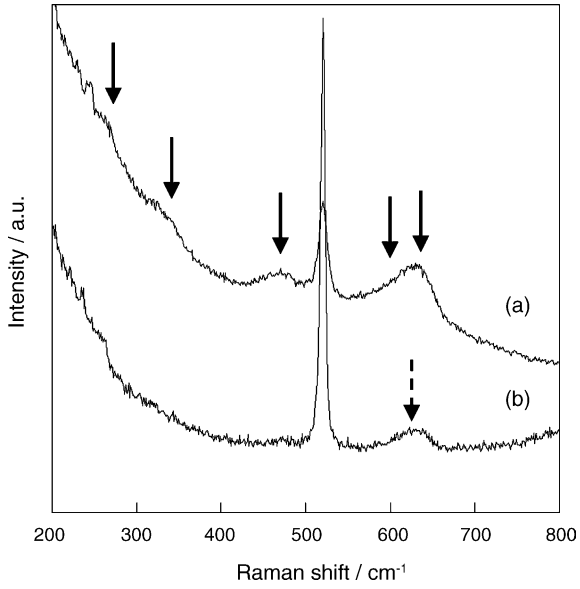

Fig. 4. Raman spectra of the Eu^{3+}-doped ZrO_2 thin film annealed at (a) 700 °C and (b) 900 °C.

the tetragonal phase of ZrO_2 [20–22]. As shown in the inset of Fig. 3, the films annealed below 700 °C show no peak shift. Thus, we concluded that tetragonal phase could be stabilized after the film was annealed below 700 °C. After the film was annealed at 900 °C, the characteristic peak corresponding to cubic phase of ZrO_2 is confirmed around 630 cm^{-1}(indicated by dashed-arrow) [20]. While, the band assigned to tetragonal or monoclinic phase could not be detected in the spectrum (b), indicates that cubic phase of ZrO_2 is stabilized at room temperature. From XRD and Raman measurement, it is concluded that phase transformation of Eu^{3+}-doped ZrO_2 thin film from tetragonal phase to cubic phase occurs between 700 and 800 °C because of the substitution of Zr^{4+} lattice site in the film by Eu^{3+} ions and formation of solid-solution.

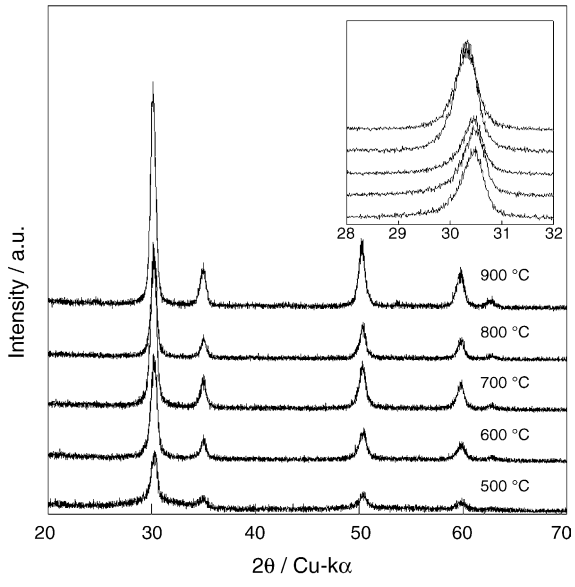

Fig. 3. XRD patterns of the Eu^{3+}-doped ZrO_2 thin film annealed at various temperatures.

The excitation spectra of Eu^{3+}-doped ZrO_2 film annealed at various temperatures are shown in Fig. 5. These excitation spectra were obtained by monitoring the emission of $^5D_0 \rightarrow {}^7F_2$ transition from Eu^{3+}. The peaks centered at 362, 380 and 396 nm are assigned to f–f transition of $^7F_0 \rightarrow {}^5D_4$, ^5G_j and $^5L_6$, respectively (Fig. 5(b)). After annealing above 500 °C, the broad band, which is due to charge transfer (CT) band between host lattice oxygen atoms and Eu, appears in the spectra. With the increase of the annealing temperature, the intensity of CT band becomes strong. While, as shown in Fig. 5(b), no changes in peak intensity can be observed in f–f transition of Eu^{3+}. The main factor affecting the intensity of the CT band is an efficiency of the energy transfer process from the CT band to the Eu^{3+} emitting level. In other words, the interaction between Eu and O orbital is very important. In this study, the obtained Eu^{3+}-doped ZrO_2 film is stabilized at cubic phase after annealing at 800 °C. The Eu–O bond length in cubic phase shows the shortest distance compared with two other well-known crystal structures (tetragonal and monoclinic), indicates that the strongest interaction affects between Eu and O. As a result, the strongest intensity of excitation peak should be obtained from the film, which has cubic structure. A blue shift of the CT band can also be observed as increasing annealing temperature. The blue shift of CT band has been reported by several researchers [23,24]. According to previous reports, the CT band position shifts to lower wavelength with the decrease of Eu–O bond length. In our film, the decrease of the Eu–O bond length can also be observed from XRD measurement. From this consideration, it is concluded that cubic phase of ZrO_2 is the optimized luminescent host. This result is in good agreement with the previous reports obtained from any other cubic-structured

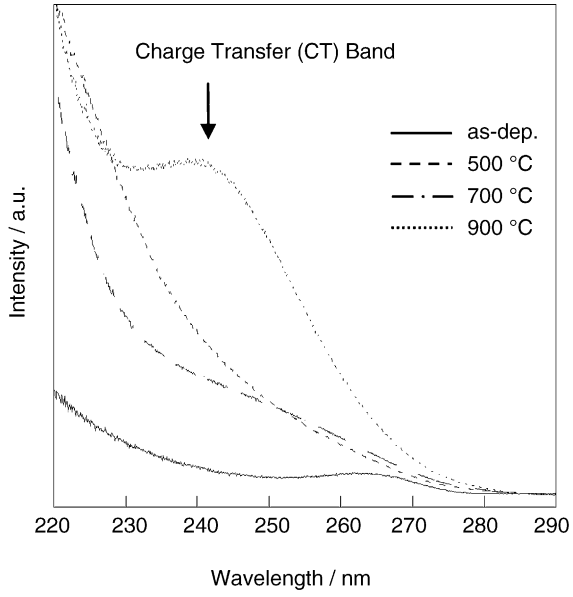

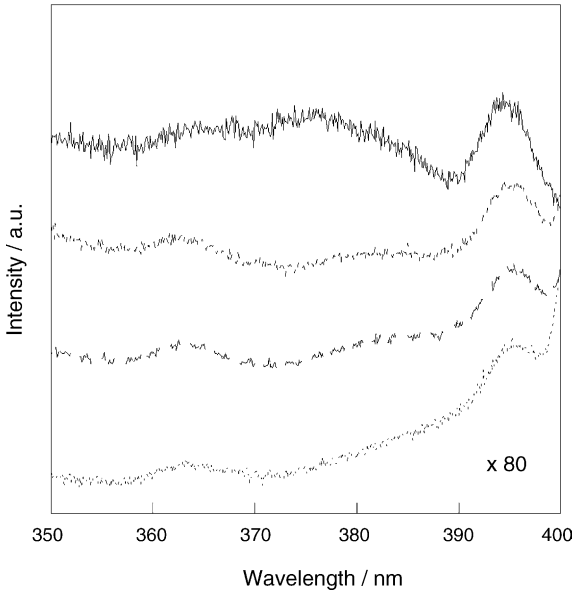

Fig. 5. Excitation spectra (monitoring the $^5D_0 \rightarrow {}^7F_2$ transition) of the Eu^{3+}-doped ZrO_2 thin film annealed at various temperatures.

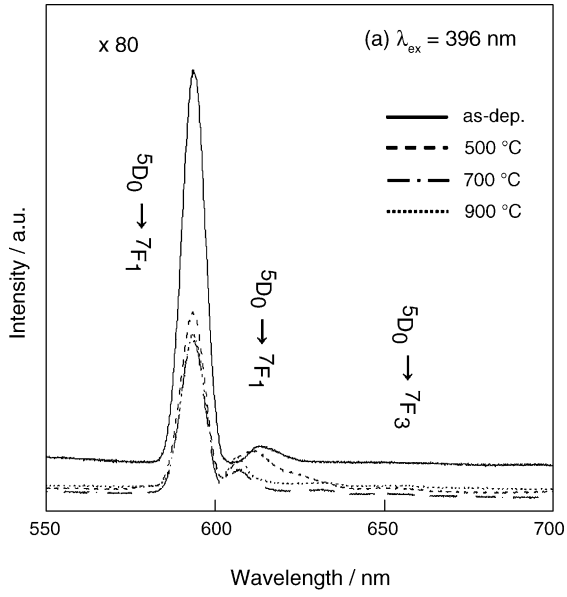

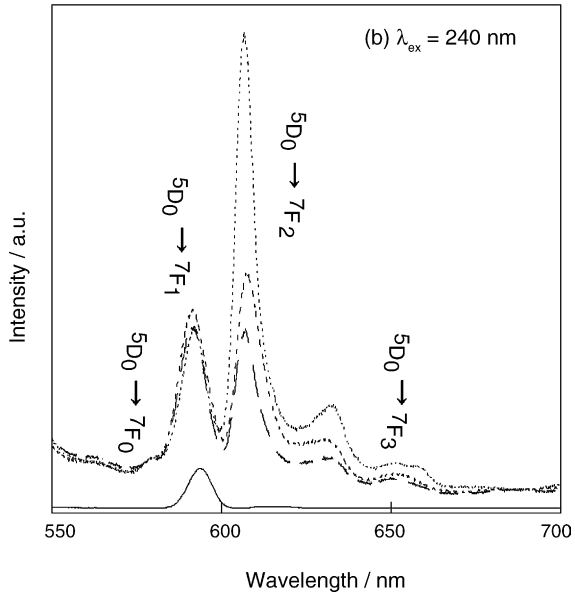

Fig. 6. Luminescence spectra of the Eu^{3+}-doped ZrO_2 thin film excited at (a) 240 nm and (b) 396 nm.

materials such as Gd_2O_3 [25] and Y_2O_3 [26]. The peak intensity of the CT band after annealed at 900 °C is about 100 times larger than that of the $^7F_0 \rightarrow {}^5L_6$ transition of Eu^{3+}.

The emission spectra of Eu^{3+}-doped ZrO_2 film excited at different wavelengths are shown in Fig. 6. The film was annealed at various temperatures. Both spectra shows characteristic red-emission peaks corresponding to $^5D_0 \rightarrow {}^7F_j$ ($j = 0$–3) transition of Eu^{3+}. If Eu^{3+} ions occupy inversion site in the lattice, the emission peak intensity of the $^5D_0 \rightarrow {}^7F_1$ transition becomes large compared with the emission peak intensity of $^5D_0 \rightarrow {}^7F_2$ transition. In our study, at 396 nm excitation, the peak intensity of $^5D_0 \rightarrow {}^7F_1$ transition is larger than that of $^5D_0 \rightarrow {}^7F_2$ transition although Eu^{3+} ions do not occupy the inversion site in the lattice, which is due to overlapping of $^5D_0 \rightarrow {}^7F_1$ and stray light from excitation light. After being annealed at 900 °C, the peak position of $^5D_0 \rightarrow {}^7F_2$ transition centered at 607 nm can be observed in both spectra. The emission peak position of Eu^{3+} is strongly related to the site symmetry of Eu^{3+} in the host lattice. Gutzov and co-workers reported that the maximum of the luminescence appeared at 607 nm because Eu^{3+} occupied D_{2h} or D_{4h} site in the cubic-structured Eu^{3+}-doped ZrO_2 material [27,28]. It is concluded that the appearance of the emission assigned to $^5D_0 \rightarrow {}^7F_2$ transition at 607 nm from deposited film is due to the site symmetry of Eu^{3+} located in the host lattice (D_{2h} or D_{4h}). The emission intensity from the film excited at 240 nm also shows strong emission peak by a factor of 100 compared with the peak intensity excited at 396 nm,

which corresponds to the difference of excitation spectra discussed in Fig. 5. This result indicates that the CT band in the film plays an important role to obtain strong emission from Eu^{3+}-doped ZrO_2 thin film fabricated by the LPD method.

4. Conclusions

We have demonstrated that high transparent Eu^{3+}-doped ZrO_2 thin films have been successfully fabricated on various kinds of substrates by the LPD method. The obtained thin films consist of densely-packed small spherical particles. The formation of solid-solution of Eu^{3+}-doped ZrO_2 thin film was observed after annealing at 800 °C. The film annealed above 800 °C showed cubic structure. Well-defined CT band could be observed from the film after annealing at 900 °C, of which intensity is about 100 times larger than the excitation peak corresponds to $^7F_0 \rightarrow {}^5L_6$ transition. It is prominent that much stronger photoluminescence intensity could be obtained from the film excited via CT band than the film excited at 396 nm.

Acknowledgement

A part of this study was supported by Grant-in-Aid for Scientific Research (A) (No. 15205026) from the Japan Society for the Promotion of Science and Grant-in-Aid for Scientific Research of Priority Areas (No. 16080211) for Panoscopic assembling and High Ordered Functions for Rare Earth Materials (440) from the MEXT in Japan.

References

[1] B. Tang, L.P. Jin, X.J. Zheng, L.Y. Zhu, Spectrochim. Acta Part A 55 (1999) 1731–1736.
[2] K. Riwotzki, M. Haase, J. Phys. Chem. B 105 (2001) 12709–12713.
[3] S.H. Byeon, M.G. Ko, J.C. Park, D.K. Kim, Chem. Mater. 14 (2002) 603–608.
[4] S.J. Yoon, P.A. Helmke, J.E. Amonette, W.F. Bleam, Langmuir 18 (2002) 10128–10136.
[5] F.S. Liu, Q.L. Liu, J.K. Liang, L.T. Yang, G.B. Song, J. Luo, G.H. Rao, J. Solid State Chem. 177 (2004) 1796–1802.
[6] M. Machida, J.I. Yabunaka, T. Kijima, Chem. Mater. 12 (2000) 812–817.
[7] S. Bernal, J.J. Calvino, G.A. Cifredo, D. Finol, J.M. Gatica, C.J. Kiely, C. López-Cartes, J.G. Zhen, H. Vidal, Chem. Mater. 14 (2002) 1405–1410.
[8] M.R. Goldwasser, M.E. Rivas, E. Pietri, M.J. Perez-Zurita, M.L. Cubeiro, L. Gingembre, L. Leclercq, Appl. Catal. A 255 (2003) 45–57.
[9] L.D. Huy, P. Laffez, Ph. Daniel, A. Jouanneaux, N.T. Khoi, D. Siméone, Mater. Sci. Eng. B 104 (2003) 163–168.
[10] P. Gao, L.J. Meng, M.P. dos Santos, V. Teixeira, M. Andritschky, Appl. Surf. Sci. 173 (2001) 84–90.
[11] T. Ngai, W.J. Qi, R. Sharma, J. Fretwell, X. Chen, J.C. Lee, S. Banerjee, Appl. Phys. Lett. 76 (2000) 502–504.
[12] M. Putkonen, L. Niinistö, J. Mater. Chem. 11 (2001) 3141–3147.
[13] K. Forsgren, J. Westlinder, J. Lu, J. Olsson, A. Hårsta, Chem. Vap. Deposition 8 (2002) 105–109.
[14] M. Cassir, F. Goubin, C. Bernay, P. Vernoux, D. Lincot, Appl. Surf. Sci. 193 (2002) 120–128.
[15] S. Deki, Y. Aoi, O. Hiroi, A. Kajinami, Chem. Lett. 25 (1996) 433–434.
[16] S. Deki, Y. Aoi, J. Okibe, H. Yanagimoto, A. Kajinami, M. Mizuhata, J. Mater. Chem. 7 (1997) 1769–1772.
[17] S. Deki, S. Iizuka, K. Akamatsu, M. Mizuhata, A. Kajinami, J. Mater. Chem. 11 (2001) 1–4.
[18] H.Y.Y. Ko, M. Mizuhata, A. Kajinami, S. Deki, J. Mater. Chem. 12 (2002) 1495–1499.
[19] S. Deki, K. Kuratani, M. Uemura, K. Akamatsu, M. Mizuhata, A. Kajinami, Thin Solid Films 460 (2004) 83–86.
[20] E.F. López, V.S. Escribano, M. Panizza, M.M. Carnasciali, G. Busca, J. Mater. Chem. 11 (2001) 1891–1897.
[21] M. Yashima, M. Kakihana, K. Ishii, Y. Ikuma, M. Yoshimura, J. Mater. Res. 11 (1996) 1410–1420.
[22] M. Li, Z. Feng, P. Ying, Q. Xin, C. Li, Phys. Chem. Chem. Phys. 5 (2003) 5326–5332.
[23] Q. Meng, J. Lin, L. Fu, H. Zhang, S. Wang, Y. Zhou, J. Mater. Chem. 11 (2001) 3382–3386.
[24] L. Sun, C. Liao, C. Yan, J. Solid State Chem. 171 (2003) 304–307.
[25] M.L. Pang, J. Lin, J. Fu, R.B. Xing, C.X. Luo, Y.C. Han, Opt. Mater. 23 (2003) 547–558.
[26] J.A. Nelson, E.L. Brant, M.J. Wagner, Chem. Mater. 15 (2003) 688–693.
[27] S. Gutzov, M. Kohls, M. Lerch, J. Phys. Chem. Solids 61 (2000) 1301–1309.
[28] S. Gutzov, M. Lerch, Opt. Mater. 24 (2003) 547–554.